Single- and two-photon wave-particle superpositions: Theory and experiment

Qing-Feng Xue,[1] Xu-Cai Zhuang,[1] Nguyen Ba An,[2,3] De-Yang Duan,[1] Ren-De Ma,[1] Wei-Wei Pan,[4] Qin-Qin Wang,[5,6] Yun-Jie Xia,[1] and Zhong-Xiao Man[1,*]

[1]*School of Physics and Physical Engineering, Shandong Provincial Key Laboratory of Laser Polarization and Information Technology, Qufu Normal University, Qufu 273165, China*

[2]*Thang Long Institute of Mathematics and Applied Sciences, Thang Long University, Nghiem Xuan Yem, Hoang Mai, Hanoi 10000, Vietnam*

[3]*Institute of Physics, Vietnam Academy of Science and Technology, 18 Hoang Quoc Viet, Cau Giay, Hanoi 10000, Vietnam*

[4]*School of Physics and Materials Engineering, Hefei Normal University, Hefei 230061, China*

[5]*CAS Key Laboratory of Quantum Information, University of Science and Technology of China, Hefei 230026, China*

[6]*CAS Center for Excellence in Quantum Information and Quantum Physics, University of Science and Technology of China, Hefei 230026, China*

(Received 20 October 2022; revised 21 June 2023; accepted 16 August 2023; published 29 August 2023)

Simultaneous observation of the wave and particle natures of a quantum object under one experimental arrangement represents the latest development regarding wave-particle duality. In this work, we propose a simple scheme using linear-optics devices to observe either the particle nature or wave nature or the wave-particle superposition (WPS) of photons by controlling a relevant classical parameter. Our setup consists of two stages, the preparation and measurement stages, with the latter stage containing an additional classical variable whose value will be given only after the first stage in order to avoid any possible communication between the two stages and thus rule out the classical hidden-variable model. We not only develop the theory but also perform the corresponding experiments. The experimental observations perfectly agree with the theoretical predictions. Our findings are the following. The frequency (wavelength) of both single- and two-photon systems is independent of whether the photon(s) is wavelike or in a WPS state, with the common fact being that the frequency (wavelength) of two photons as a whole entity is twice (half) that of a single photon. As for the interference-pattern visibility, it is always lower in the case of WPS than in the case of a wavelike state for a single photon as well as for two photons. Remarkably, with a given value of the control parameter, the interference visibility in the case of WPS is always higher in the single-photon scenario than in the two-photon one. Although here we are dealing with photons, the obtained results apply equally well to matter particles.

DOI: 10.1103/PhysRevA.108.022223

I. INTRODUCTION

Understanding the nature of quantum objects' behaviors is the premise for a reasonable description of the quantum world. Depending on whether the interference can be produced or not, the quantum object is endowed with dual features of a wave and a particle, i.e., the so-called wave-particle duality (WPD), which are generally observed in the so-called mutually exclusive experimental arrangements in the sense of Bohr's complementarity principle [1]. The confirmation of WPD in the early days of quantum theory is mostly based on diffraction or double-slit-type experiments of matter particles, such as electrons, atoms, neutrons, and so on [2–5]. The Mach-Zehnder interferometer (MZI), being almost equivalent to the double-slit-type setup, is also widely used to illustrate the WPD of photons and electrons. In the case of the MZI, one usually resorts to the existence or absence of the second beam splitter (BS) to reveal the wave or particle character of a photon. After having been split by the first BS, the photon is prepared in a quantum superposed state of two paths, which will collapse into either path if the detection is made directly at the ends of individual paths in the absence of the second BS, indicating the particle nature of the photon. In contrast, if the two paths are recombined by the second BS before detection, interference fringes appear, showing the wave property of the photon. Here, interference means the dependence of the photon detection probability on the difference in the two optical paths brought about by phase shifters placed on the photon paths. Since the behaviors of a photon are always concomitant with the configurations of experimental setup, one might envisage that the photon could adapt its behaviors in advance to the foregoing setting. In order to exclude such a classical hidden-variable model (HVM), Wheeler proposed a delayed-choice experiment in which the second BS is randomly chosen to be inserted or removed after the photon has already passed the first BS of the MZI but is still on the way to the second BS [6]. Subsequent experiments showed that similar results can be acquired for both normal and delayed-choice situations, consistent with quantum-mechanical predictions [7].

A quantum version of the delayed-choice experiment was suggested in Ref. [8], where the second BS could be in a superposition of presence and absence via coherent quantum control of an ancilla. With this setting, the photon can be

*Corresponding author: zxman@qfnu.edu.cn

forced into a superposed state of the particle and wave and exhibits continuous morphing between those two sides with changing the controlling parameter of the ancilla. Moreover, the complementary properties of a photon can be measured in a single experimental setup by correlating the measurement outcome of the ancilla after the photon has already been detected, reversing the temporal order of the measurements. This type of postchoice of the second BS being present or absent also relaxes the requirement of ultrafast switch in the classical delayed-choice experiment. An experimental realization of this quantum delayed-choice setup with a single photon was done in Ref. [9] by taking the polarization state of the photon itself as the ancilla. In Ref. [10], a two-photon quantum delayed-choice experiment was performed using an integrated photonic device, in which one photon acts as a system and the other one acts as an ancilla. Other realizations of the quantum delayed-choice experiment were successfully implemented in different contexts [11–20].

In order to rule out classical HVMs, the delayed-choice process is generally required through either inserting or removing the second balanced beam splitter (BBS) randomly as in Wheeler's original delayed-choice experiment [6] or applying a quantum BBS in the superposition state of the presence and absence controlled by an ancilla, as proposed in Ref. [8]. However, being based on wave-particle objectivity, these possible methods have been shown to be self-inconsistent, and the predictions of quantum mechanics can be reproduced by means of the classical two-dimensional nonretrocausal HVM [21]. Fortunately, this proves that a slight modification of Wheeler's delayed-choice experiment can exclude the HVM. Namely, instead of being inserted or removed randomly, the second BBS can simply be displaced, corresponding to introducing an additional phase in a delayed manner [21]. This proposal can be demonstrated concretely with the device-independent preparation-and-measurement (PAM) scenario through the violation of the dimension witness [21,22] and has been realized in experiment [23–26].

In this work, following the method in Ref. [21], we design and implement an experimental setup to observe the wave-particle superposed state of a photon without using quantum control or entanglement assistance. Our distinct scheme is based on the combination of two complementary events, namely, whether to monitor the photon in the path of the MZI or not. It is known that the photon is bound to manifest a particle feature if the path information is exposed by, for example, inserting an opaque object in one path of the MZI to absorb or scatter the photon. Without this object, or, alternatively, with a transparent one in the path, the photon will exhibit the wave property. Instead of the opaque or transparent object, the use of a semitransparent one such as an unbalanced BS would induce the photon wave-particle superposition (WPS). Here, we show that the photon exhibits WPS when it does not interact with the semitransparent object (i.e., the object is not detected by the photon); otherwise, it behaves as a particle. Although we place objects with different transmissivities in the optical path to induce the wavelike, particlelike, and WPS-like properties of a photon, the detection results in terms of interference fringes can, in turn, signal the transmissivities of the object, similar to the counterfactual protocol called interaction-free measurement (IFM) [27–33]. The connection between WPD and IFM represents a potential application of our scheme in quantum imaging which is well suited to detecting fragile objects [33].

The superposition of the dual natures of a photon represents a milestone of the development of WPD and deepens our understanding of the fundamental laws of quantum mechanics [34–41]. In previous works [8–15], WPS observations were mostly made for single photons and were less explored for multiphoton situations. As is known, the wavelength of an N-photon state is simply λ/N, with λ being the single-photon state wavelength, which is equivalent to the matter de Broglie wavelength of all N photons as one entity [42]. Therefore, the wave property of an N-photon state can be characterized with an interference fringe that is N times finer than the conventional fringe of a single photon [43–46]. However, the pattern of the interference fringe of N photons being in WPS has not yet been addressed in detail. In particular, questions such as whether this N times relation still holds with respect to the interference fringe of an entire set of N photons being in a WPS state and what the interference visibility of an N-photon WPS state is compared with the corresponding purely wavelike one depending on N need to be demystified. In this work, we also implement the two-photon experiment, and our results show that, as in the purely wavelike scenario, in the scenario of WPS the interference fringe of two photons is also 2 times finer than that of a single photon.

This paper is organized as follows. In Sec. II, we present our experimental setup and develop the underlying theory. The setup is designed such that not only can the photon WPS behaviors be observed but also the classical HVM can be abandoned. The theoretical predictions obtained in Sec. II are tested experimentally in Sec. III. Conclusions are made in Sec. IV.

II. THEORY

Our setup with the PAM scenario is depicted in Fig. 1, which consists of the preparation and measurement stages, denoted by two shaded parts. In the preparation stage, a BS with transmissivity $\cos^2\alpha$ (with $0 \leqslant \alpha \leqslant \pi/2$ considered to be a classical control parameter) is inserted in path A of the MZI, a detector D_E is used to detect a possible photon in path E, and a phase shifter in path B is introduced to provide a variable value of the phase φ. In the measurement stage, an extra phase shifter ϕ is inserted in path A, which should be placed after the preparation one to exclude possible correlations between these two stages. The tunable BS is tantamount to "nothing," or a 100% transparent object, for $\alpha = 0$ and to a mirror for $\alpha = \pi/2$, whereas for $0 < \alpha < \pi/2$ it serves as an opaque object which partly transmits and partly reflects the incoming signal. As a result, a photon behaves as a wave when $\alpha = 0$ and as a particle when $\alpha = \pi/2$. Being confined between these two extreme values, i.e., $0 < \alpha < \pi/2$, the photon will be forced to a superposition of the wave and particle (i.e., they are at the same time both wavelike and particlelike) if D_E does not fire.

In this section we theoretically formulate our scheme as follows. A single photon is sent from path a with the input state $|\psi_{\rm in}^{(1)}\rangle_{abE} = |100\rangle_{abE}$, with $|lmn\rangle_{xyz} \equiv |l\rangle_x \otimes |m\rangle_y \otimes |n\rangle_z$ denoting the l, m, and n photons in paths x, y, and z,

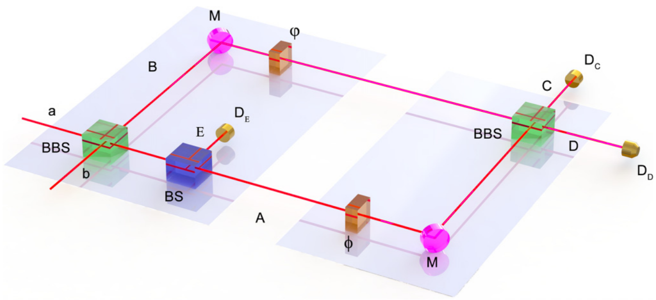

FIG. 1. Schematic of our experimental setup using the MZI for observations of WPS of photons. The two shaded parts correspond to two stages of the experiment: the stage of preparation (left part) and the stage of measurement (right part). A beam splitter (BS) is inserted in path A, and two balanced beam splitters (BBSs) are the input and output of the MZI. Photodetectors D_E, D_C, and D_D are used to detect possible photons in paths E, C, and D, respectively. Two phase shifters are used: one is placed on path B in the preparation stage to provide a variable phase φ, and the other one is placed on path A in the measurement stage to provide another variable phase ϕ. The value of ϕ will be given after the value of φ with the purpose being to rule out the two-dimensional HVM (see text). M denotes the mirror. For the single-photon scenario a photon is injected via port a, while for the two-photon scenario one photon is input to port a and, simultaneously, the other one is input to port b.

respectively, and the superscript (1) denoting the case of a single photon. A straightforward calculation yields an output state of the form

$$\left|\psi_{\text{out}}^{(1)}\right\rangle_{CDE} = \left(\cos\alpha\left|\psi_w^{(1)}\right\rangle_{CD} + \frac{\sin\alpha}{\sqrt{2}}\left|\psi_p^{(1)}\right\rangle_{CD}\right)|0\rangle_E + \frac{\sin\alpha}{\sqrt{2}}|00\rangle_{CD}|1\rangle_E, \tag{1}$$

where

$$\left|\psi_w^{(1)}\right\rangle_{CD} = e^{i(\varphi-3\phi)/2}\left[\sin\frac{\varphi-\phi}{2}|10\rangle_{CD} - i\cos\frac{\varphi-\phi}{2}|01\rangle_{CD}\right] \tag{2}$$

and

$$\left|\psi_p^{(1)}\right\rangle_{CD} = -\frac{i}{\sqrt{2}}e^{i\varphi}(|10\rangle_{CD} + |01\rangle_{CD}) \tag{3}$$

are the wave and particle states of a photon, operationally representing the capacity and incapacity to produce interference in terms of the (φ, ϕ) dependence of the photon detection probability, respectively. Note that the wave and particle states are not orthogonal to each other since $\langle\psi_p^{(1)}|\psi_w^{(1)}\rangle = \frac{1}{\sqrt{2}}e^{-2i\phi}$. With a probability of $\frac{1}{2}(1+\cos^2\alpha)$ the detector D_E is silent, and state $|\psi_{\text{out}}^{(1)}\rangle_{CDE}$ (1) collapses into

$$\left|\psi_{wp}^{(1)}\right\rangle_{CD} = \frac{1}{\sqrt{1+\cos^2\alpha}}\left[\sqrt{2}\cos\alpha\left|\psi_w^{(1)}\right\rangle_{CD} + (1-\cos\alpha)\left|\psi_p^{(1)}\right\rangle_{CD}\right], \tag{4}$$

which is a single-photon WPS; that is, the photon behaves at the same time as a wave and a particle. Hence, the photon will manifest a pure particle nature or WPS depending on whether the detector D_E responds. Since we are interested in the observation of WPS of the photon, we restrict measurement outcomes to the subspace where D_E does not fire.

The probability that detector D_C or D_D clicks can be expressed as

$$P_C^{(1)} = \tfrac{1}{4}[1+\cos^2\alpha - 2\cos\alpha\cos(\varphi-\phi)] \tag{5a}$$

$$= \cos^2\alpha P_C^{w,(1)} + (1-\cos\alpha)^2 P_C^{p,(1)} + 4\cos\alpha(1-\cos\alpha)P_C^{w,(1)}P_C^{p,(1)} \tag{5b}$$

or

$$P_D^{(1)} = \tfrac{1}{4}[1+\cos^2\alpha + 2\cos\alpha\cos(\varphi-\phi)] \tag{6a}$$

$$= \cos^2\alpha P_D^{w,(1)} + (1-\cos\alpha)^2 P_D^{p,(1)} + 4\cos\alpha(1-\cos\alpha)P_D^{w,(1)}P_D^{p,(1)}, \tag{6b}$$

where $P_C^{w,(1)} = \sin^2[(\varphi-\phi)/4]$, $P_D^{w,(1)} = \cos^2[(\varphi-\phi)/4]$, and $P_C^{p,(1)} = P_D^{p,(1)} = \frac{1}{4}$ are contributions of the particle and wave components of the photon to the total detecting probabilities of D_C and D_D, with the superscript p (w) implying particle (wave). Interestingly, the third terms in Eqs. (5b) and (6b) indicate visually that the probabilities $P_C^{(1)}$ and $P_D^{(1)}$ are also contributed by the quantum interference of the wave and particle natures of the photon, implying that the photon is in a pure state of WPS once it is detected in D_C or D_D.

In order to rule out the classical HVMs, we have adopted the method proposed in Refs. [21,22] by introducing an additional phase ϕ in the measurement stage, with its value being given after the photon has passed the preparation stage. Since the photon has two spatial modes with two detection results, four values can be set for φ (i.e., $\varphi_0, \varphi_1, \varphi_2, \varphi_3$), and two can be set for ϕ (i.e., ϕ_0, ϕ_1) [21,22]. The matrix to test the dimension witness reads [47]

$$W_2 = \begin{bmatrix} p(0,0)-p(1,0) & p(2,0)-p(3,0) \\ p(0,1)-p(1,1) & p(2,1)-p(3,1) \end{bmatrix}, \tag{7}$$

in which $p(x,y) = p(D_C = 1|\varphi_x, \phi_y)$ is the probability that D_C fires for the combination of φ_x and ϕ_y. For the state (1), we derive that $p(x,y) = [1+\cos^2\alpha - 2\cos(\varphi_x - \phi_y)\cos\alpha]/2(1+\cos^2\alpha)$. By plotting $|\text{Det}(W_2)|$ against φ and α in Fig. 2(a), we can see that $|\text{Det}(W_2)| > 0$ in several areas; that is, the dimension witness is violated, which rules out the possibility of HVMs. In our setup, we set α to 0.176π and choose the values of φ_x and ϕ_y to be $\varphi_0 = 0$, $\varphi_1 = \pi$, $\varphi_2 = -\pi/2$, $\varphi_3 = \pi/2$, and $\phi_0 = \pi/2$, $\phi_1 = 0$. In this case, the quantum probabilities give rise to $|\text{Det}(W_2)| = 0.974$, implying the violation of classical prediction. In the experiment, we obtained $|\text{Det}(W_2)| = 0.907 \pm 0.003$ by postselecting only those events where a signal photon and a trigger photon arrived simultaneously. The above analysis of $|\text{Det}(W_2)|$ actually does not take into account the mutual influences among noise terms as well as their effects on the hidden variables [21]. To exclude such an effect, one can adopt the linear

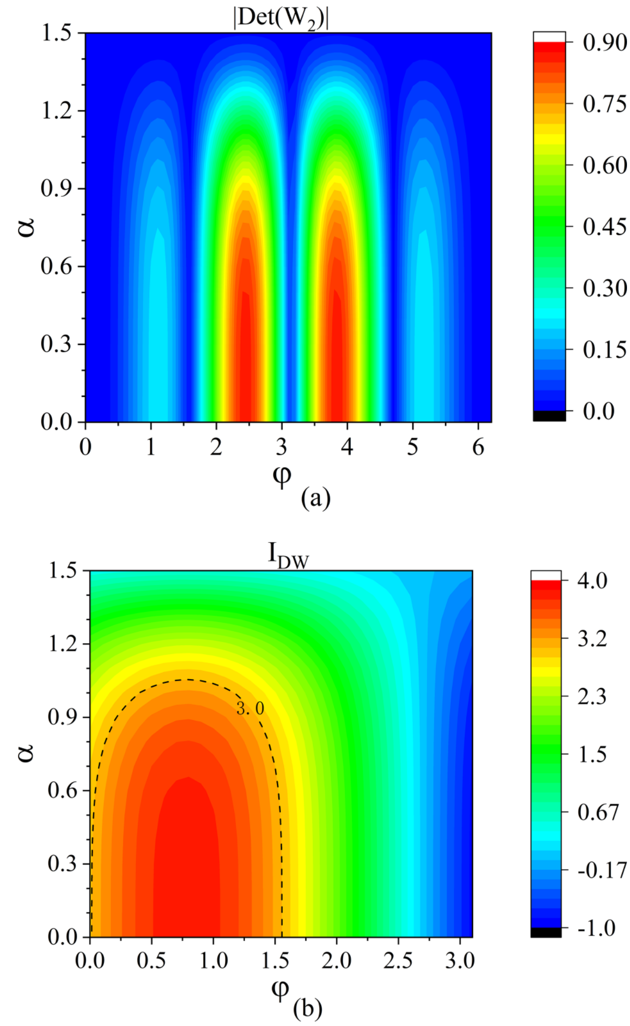

FIG. 2. (a) The contour plots of the dimension witness $|\mathrm{Det}(W_2)|$ as a function of φ and α for the choice of $\varphi_0 = \varphi_1/2 = \varphi_2/3 = \varphi_3/4 = \varphi$, $\phi_0 = 0$, and $\phi_1 = \pi/2$. (b) The contour plots of the linear dimension witness I_{DW} as a function of φ and α for the choice of $\varphi_0 = -\varphi_1 = \varphi$, $\varphi_2 = \pi$, $\phi_0 = 0$, and $\phi_1 = \pi/2$. The region of $I_{\mathrm{DW}} > 3$ is surrounded by the dashed line, inside which the dimension witness is violated. The existence of the region of $I_{\mathrm{DW}} > 3$ implies the irrelevance of the HVMs.

dimension witness formulated in an inequality form as [48]

$$I_{\mathrm{DW}} = \langle D_{00}\rangle + \langle D_{01}\rangle + \langle D_{10}\rangle - \langle D_{11}\rangle - \langle D_{20}\rangle \leqslant 3, \quad (8)$$

where $\langle D_{xy}\rangle = p(D_D = 1|\varphi_x, \phi_y) - p(D_C = 1|\varphi_x, \phi_y)$ is the probability difference between D_D and D_C to detect a photon. From Fig. 2(b), we can see the regions with $I_{\mathrm{DW}} > 3$, indicating the violation of the linear dimension witness. In our setup, when α is chosen to be 0.176π, the values of φ_x and ϕ_y are set as $\varphi_0 = 7\pi/4$, $\varphi_1 = 5\pi/4$, $\varphi_2 = \pi/2$, and $\phi_0 = \pi/2$, $\phi_1 = 0$. The theoretical and experimental values of I_{DW} are 3.779 and 3.660 ± 0.007, respectively.

To make a comparison with the properties of one photon, in particular where the WPS is concerned, we also present the results for two photons, with each of them being sent through a path of a and b with the input state $|\psi^{(2)}_{\mathrm{in}}\rangle_{abE} = |110\rangle_{abE}$. The output state can be derived as

$$\begin{aligned}\big|\psi^{(2)}_{\mathrm{out}}\big\rangle_{CDE} = {} & \left(\cos^2\alpha\big|\psi^{(2)}_w\big\rangle_{CD} + \sqrt{\frac{1-\cos^4\alpha}{2}}\big|\psi^{(2)}_p\big\rangle_{CD}\right)|0\rangle_E \\ & + \frac{i\cos\alpha\sin\alpha}{\sqrt{2}}(|10\rangle_{CD} - |01\rangle_{CD})|1\rangle_E \\ & + \frac{\sin^2\alpha}{\sqrt{2}}|00\rangle_{CD}|2\rangle_E, \end{aligned} \quad (9)$$

where

$$\big|\psi^{(2)}_w\big\rangle_{CD} = e^{i\varphi}\left[\frac{i\sin\varphi}{\sqrt{2}}(|20\rangle_{CD} + |02\rangle_{CD}) + \cos\varphi|11\rangle_{CD}\right] \quad (10)$$

and

$$\big|\psi^{(2)}_p\big\rangle_{CD} = \tfrac{1}{2}e^{i2\varphi}(|20\rangle_{CD} + \sqrt{2}|11\rangle_{CD} + |02\rangle_{CD}) \quad (11)$$

are the wave and particle states of the two photons, respectively, with the superscript (2) indicating the scenario with two photons. Note also that the two-photon wave and particle states are not orthogonal to each other since $\langle\psi^{(2)}_p|\psi^{(2)}_w\rangle = \frac{1}{\sqrt{2}}$. For clarity, in the case of two photons, we set the extra phase to $\phi = 0$ since it can be absorbed into the total phase. With a probability of $\frac{1}{2}(1 + \cos^4\alpha)$ the detector D_E is silent, and $|\psi^{(2)}_{\mathrm{out}}\rangle_{CDE}$ collapses into

$$\begin{aligned}&\big|\psi^{(2)}_{w-p}\big\rangle_{CD} \\ &\quad = \frac{1}{\sqrt{1+\cos^2\alpha}}\left(\sqrt{2}\cos\alpha\big|\psi^{(2)}_w\big\rangle_{CD} + \sin\alpha\big|\psi^{(2)}_p\big\rangle_{CD}\right),\end{aligned} \quad (12)$$

which is a WPS; that is, the two photons as a whole exhibit both particle and wave behavior at the same time.

Let us denote $P^{(2)}_{C(D)}$ as the probability that only detector $D_{C(D)}$ clicks, while $P^{(2)}_{CD}$ is the joint probability that both D_C and D_D respond simultaneously. These detecting probabilities can be formulated as

$$P^{(2)}_{C(D)} = \tfrac{1}{2}\cos^2\alpha\sin^2\varphi + \tfrac{1}{8}\sin^4\alpha \quad (13a)$$

$$\begin{aligned}&= \cos^4\alpha P^{w,(2)}_{C(D)} + \sin^4\alpha P^{p,(2)}_{C(D)} \\ &\quad + 8\cos^2\alpha\sin^2\alpha P^{p,(2)}_{C(D)}P^{w,(2)}_{C(D)},\end{aligned} \quad (13b)$$

$$P^{(2)}_{CD} = \cos^2\alpha\cos^2\varphi + \tfrac{1}{4}\sin^4\alpha \quad (14a)$$

$$\begin{aligned}&= \cos^4\alpha P^{w,(2)}_{CD} + \sin^4\alpha P^{p,(2)}_{CD} \\ &\quad + 4\cos^2\alpha\sin^2\alpha P^{p,(2)}_{CD}P^{w,(2)}_{CD},\end{aligned} \quad (14b)$$

where $P^{w,(2)}_C = P^{w,(2)}_D = \frac{1}{2}\sin^2\varphi$ and $P^{p,(2)}_C = P^{p,(2)}_D = \frac{1}{8}$ are the contributions of the wave and particle features of the two photons to $P^{(2)}_C$ and $P^{(2)}_D$, while $P^{w,(2)}_{CD} = \cos^2\varphi$ and $P^{p,(2)}_{CD} = \frac{1}{4}$ represent those of the two photons to the joint probability $P^{(2)}_{CD}$. We see that the quantum interference effects of the wave and particle components of the two photons are recognized by the third terms in Eqs. (13b) and (14b), which occurs when $0 < \alpha < \pi/2$. The expressions for $P^{(2)}_{C(D)}$ and $P^{(2)}_{CD}$ also show that, when $\alpha = 0$, the two photons as an entity are 100% wavelike and, when $\alpha = \pi/2$, they are 100% particlelike.

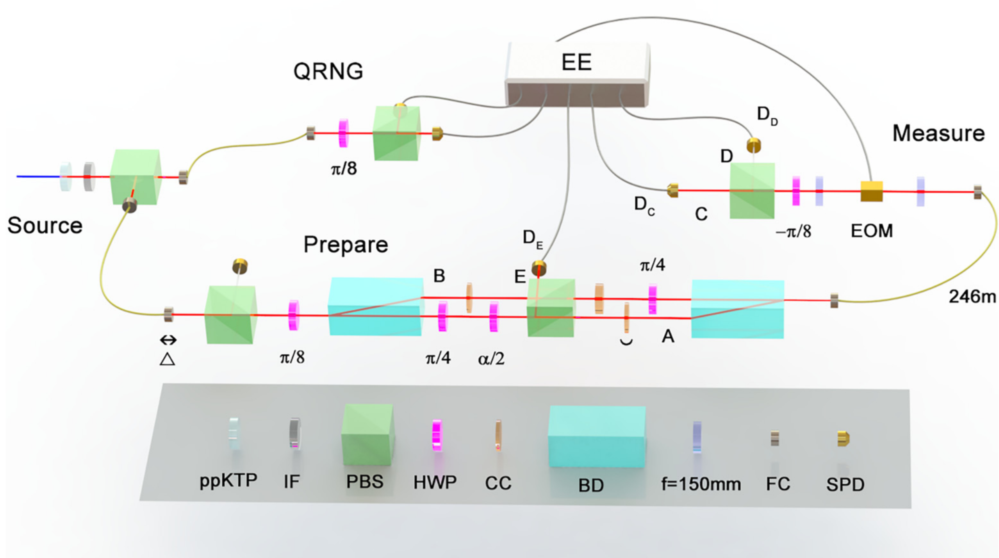

FIG. 3. Experimental setup for observations of various photon behaviors. In the experiment for a single photon, one of the generated photons (trigger) is sent to the quantum random number generation (QRNG) station to select a phase shift ϕ between 0 and $\frac{\pi}{2}$. The second photon (signal) enters the delay-choice interferometer, which consists of two parts corresponding to the preparation and measurement stages. For the two-photon experiment, each of the two photons is injected into a port of the setup. Δ is the delay introduced between the H and V polarizations of the photon. The legend displays the periodically poled potassium titanium phosphate (PPKTP) nonlinear crystal, interference filter (IF), polarization beam splitter (PBS), half-wave plate (HWP), compensated crystal (CC), beam displacer (BD), convex lens ($f = 150$ mm), fiber collimator (FC), and single-photon detector (SPD).

From Eqs. (5a)–(6b) and (13a)–(14b) it follows that for $0 \leqslant \alpha < \pi/2$ the detecting probabilities are $P_C^{(1)} \sim \cos^2(\varphi/2)$ $[P_D^{(1)} \sim \sin^2(\varphi/2)]$ in the single-photon case and $P_{C,D}^{(2)} \sim \sin^2\varphi$ and $P_{CD}^{(2)} \sim \cos^2\varphi$ in the two-photon one. Analyzing the full formulas of the probabilities, we come up with two main theoretical predictions; one is regarding the frequency (wavelength) of oscillation of the probabilities as a function of the phase φ, and the other concerns the visibilities of the interference patterns. First, the probabilities associated with the WPS states (i.e., when $0 < \alpha < \pi/2$) under both the single- and two-photon situations oscillate versus φ with the same frequencies (wavelengths) as those known for photons exhibiting a purely wave nature (i.e., when $\alpha = 0$) [43]. However, the oscillation frequency (wavelength) under the two-photon situation is twice (half) that under the single-photon one. Second, we deal with the visibilities of interference patterns defined as $V^{(1)} = (\max P_{C,D}^{(1)} - \min P_{C,D}^{(1)})/(\max P_{C,D}^{(1)} + \min P_{C,D}^{(1)})$ in the single-photon scenario and $V^{(2)} = (\max P_{CD}^{(2)} - \min P_{CD}^{(2)})/(\max P_{CD}^{(2)} + \min P_{CD}^{(2)})$ in the two-photon scenario. In terms of the control parameter α, analytical expressions for the visibilities read

$$V^{(1)} = \frac{1}{1+\upsilon^{(1)}}, \qquad V^{(2)} = \frac{1}{1+\upsilon^{(2)}}, \tag{15}$$

with

$$\upsilon^{(1)} = \frac{2\sin^4(\alpha/2)}{\cos\alpha}, \qquad \upsilon^{(2)} = \frac{\sin^4(\alpha)}{2\cos^2\alpha}. \tag{16}$$

At $\alpha = 0$ (purely wavelike behavior) we have $\upsilon^{(1)} = \upsilon^{(2)} = 0$, so $V^{(1)} = V^{(2)} = 1$, implying perfect visibility independent of the considered number of photons. At $\alpha = \pi/2$ both $\upsilon^{(1)}$ and $\upsilon^{(2)}$ are infinite, so $V^{(1)} = V^{(2)} = 0$, implying a particlelike nature without any interference patterns. Interestingly, in the WPS states with $0 < \alpha < \pi/2$ it can be verified using the properties of trigonometric functions that $1 - (\upsilon^{(1)}/\upsilon^{(2)}) = [2\cos^2(\alpha/2) + \cos^2\alpha]/(1+\cos\alpha)^2$, which is obviously always positive. This is tantamount to the inequality $\upsilon^{(2)} > \upsilon^{(1)}$, which in turn means $V^{(2)} < V^{(1)}$. That is, when the photons are in WPS states the two-photon interference-pattern visibility is always lower than the single-photon one. Also, in the entire relevant range of variation of α (i.e., $0 \leqslant \alpha < \pi/2$) both $\upsilon^{(1)}$ and $\upsilon^{(2)}$ increase with α. This fact predicts that the interference visibilities $V^{(1)}$ and $V^{(2)}$ decrease with increasing α due to the decreased weights of the wavelike components in the WPS states of both single- and two-photon cases. In the next section we shall carry out experiments to examine whether the above-mentioned theoretical predictions are justified.

III. EXPERIMENT

Our experimental arrangements are detailed in Fig. 3, where a continuous-wave laser (with a central wavelength of 405 nm) is used to generate photon pairs (with a central wavelength of 810 nm) from a periodically poled potassium titanium phosphate (PPKTP) nonlinear crystal via spontaneous parametric down-conversion processes. To implement the single-photon experiment, the horizontally polarized single photon (trigger) is sent to the quantum random-number-generation (QRNG) station, while the vertically polarized one (signal) is sent to the interferometer.

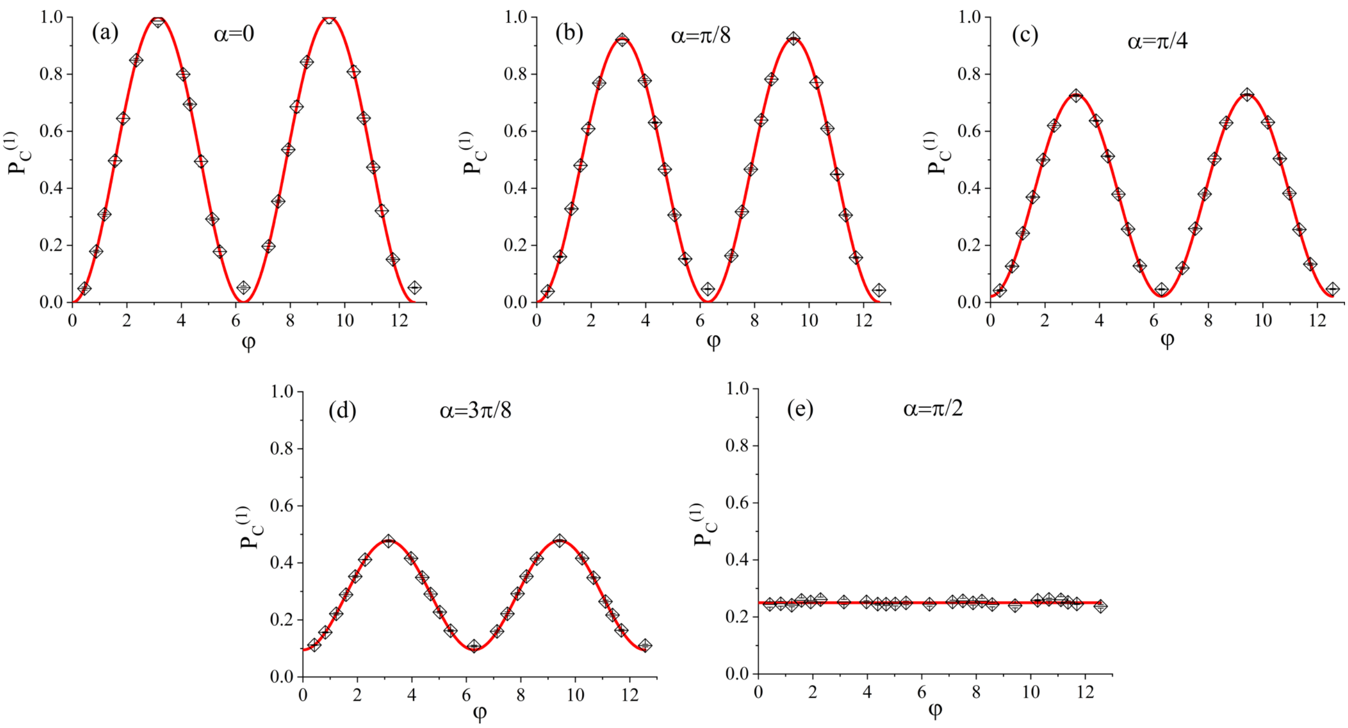

FIG. 4. The detecting probabilities $P_C^{(1)}$ of the single-photon case with respect to the phase φ for different α. The black symbols are experimental results, and the lines are corresponding theoretical ones.

In the QRNG station, after a half-wave plate (HWP) at $\frac{\pi}{8}$, the polarization of the photon is rotated to $|+\rangle = (|H\rangle + |V\rangle)/\sqrt{2}$, which then enters a polarization beam splitter (PBS). Here and throughout the paper, H and V denote the horizontal and vertical polarizations of the photon, respectively. The detecting probabilities of horizontally and vertically polarized photons should be the same. Photons are converted into electrical signals through a single-photon detector, and the electrical signals are divided into two channels through a BNC tee adapter. One of the signals is modulated by an arbitrary wave-form generator and a high-voltage amplifier to trigger the electro-optic modulator (EOM). Another signal is connected to a time-to-digital converter (ID Quantique, ID800). In Fig. 3, we use electrical equipment (EE) to refer to the electrical instruments mentioned above.

The interferometer station is further divided into preparation and measurement stages. In the preparation stage, we use three compensated crystals, two of which are applied to compensate the optical path, and the remaining one is rotated at an angle to introduce a variable single-photon phase shift φ by moving the displacement table. We set HWPs at $\frac{\pi}{8}$ and $-\frac{\pi}{8}$ to ensure the possible interference and another two HWPs at $\frac{\pi}{4}$ for bit inversion. The HWP at $\frac{\alpha}{2}$ can be adjusted at any angle $0 \leqslant \alpha \leqslant \pi/2$ to act as a polarizer, transforming the photon state $a_H^\dagger|0\rangle_A$ to $\cos\alpha a_H^\dagger|0\rangle_A + \sin\alpha a_V^\dagger|0\rangle_A$. If we set $\alpha = 0$ ($\alpha = \pi/2$), the photon in path A is horizontally (vertically) polarized, and the PBS is equivalent to nothing (a mirror), so that the single photon exhibits wavelike (particlelike) behavior. Between these two extreme cases, the setting of $0 < \alpha < \pi/2$ causes a superposed state of the wave and particle of the single photon when the detector D_E does not fire. In the measurement stage, to ensure the delayed choice, the signal photon is delayed by 1230 ns through a 246-m-long optical fiber. The signal photon is then focused by a convex lens pair (focal length $f = 150$ mm) into the spatial EOM. Considering the rise and fall time of the arbitrary wave-form generator (8.4-ns minimum, 100-ps resolution) and the slew rate of the high-voltage amplifier (400 V/μs), the choice of measurement stage needs a response time of around 722 ns, which is shorter than the delay time after the phase is applied on path B in the preparation stage. By setting the output voltage of the high-voltage amplifier to change the refractive index of the electro-optic modulator, we choose two phase shifts corresponding to 0 and $\frac{\pi}{2}$. In the experiment, we selected only the time when both signal and trigger photons arrived simultaneously.

In Figs. 4(a)–4(e), in terms of the dependence of $P_C^{(1)}$ on φ, we demonstrate transitions of behaviors of the single photon from wavelike to particlelike by choosing $\alpha = j\pi/8$, with $j = 0, 1, 2, 3, 4$. The black symbols are experimental results, and the curves are corresponding theoretical fits obtained from Eq. (5a) or Eq. (5b). We can see that the experimental data points are in good agreement with the theoretical curves. For $\alpha = 0$, as shown in Fig. 4(a), we observe an oscillation with a high visibility of 0.951, indicating that the single photon exhibits a purely wave property. For $\alpha = \pi/2$, as shown in Fig. 4(e), the detection probability remains 0.25 with a very low visibility of 0.024, signaling the entirely particle behavior of the photon. As α increases from 0 to $\pi/2$, the photon, being in the WPS state, exhibits a continuous transition of its behavior from wavelike to particlelike, as seen in Figs. 4(b)–4(d), both experimentally and theoretically.

Next, we turn to the observation of two-photon WPS and compare it with the case with a single photon. We connect

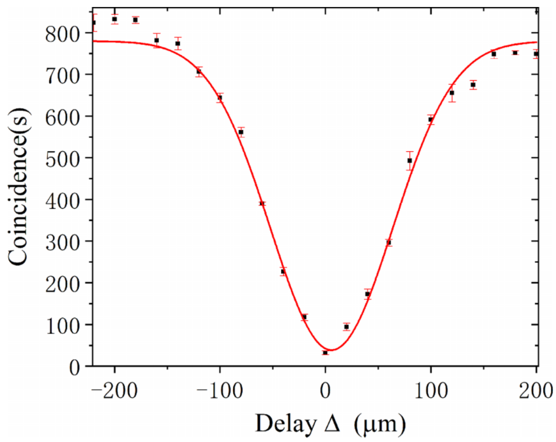

FIG. 5. Two-photon coincidence as a function of the relative delay Δ between the H and V polarizations. The integration time of each point is 1s and the visibility of the fitting curve is 0.94.

trigger photons to the input of the interferometer through a fiber-optic collimator. In order to make the two photons indistinguishable, we set the HWP in the preparation stage ($\frac{\pi}{8}$ in the single-photon experiment) to zero, while keeping the other HWPs in the interferometer unchanged. The fiber coupler for the H-polarized photon is mounted on a micro-translation stage to introduce a delay Δ between the H and V polarizations. Two-photon coincidence counts are registered to measure the probability that D_C and D_D have detected a photon at the same time, which is shown in Fig. 5. Figure 5 shows the typical Hong-Ou-Mandel dip with a visibility of 0.94 and a full width at half height of 201.88 μm, which are derived from a least-squares fit to a mathematically convenient Gaussian shape (the red solid curve). The less than 100% visibility is a result of the imperfect spatial mode match between the pairs of down-converted photons.

Having confirmed the indistinguishability of two photons, we implement the experiment to observe two-photon WPS by setting the delay Δ at the bottom of the dip in Fig. 5. The same as in the single-photon experiment, we set HWPs at the preparation and measurement stages to $\frac{\pi}{8}$ and $-\frac{\pi}{8}$, respectively, and perform bit inversion on the other two HWPs at $\frac{\pi}{4}$. The HWP at $\frac{\alpha}{2}$ can be adjusted at any angle $0 \leqslant \alpha \leqslant \pi/2$ to act as a polarizer, which transforms the two-photon state $a_H^{\dagger 2}|0\rangle_A$ to $(\cos\alpha a_H^\dagger + \sin\alpha a_V^\dagger)^2|0\rangle_A$. If we set $\alpha = 0$ $(\alpha = \pi/2)$, the two photons in path A are horizontally (vertically) polarized, and PBS2 amounts to nothing (a mirror), so that the two photons exhibit wave (particle) properties. Of interest is the setting of $0 < \alpha < \pi/2$, under which we can obtain a superposed state of waves and particles of the two photons when the detector D_E is silent.

In Figs. 6(a)–6(e), in terms of the dependence of the joint detecting probability $P_{CD}^{(2)}$ on φ, we demonstrate the wave-to-particle transitions of behaviors of the two photons by choosing $\alpha = j\pi/8$, with $j = 0, 1, 2, 3, 4$. The experimental data points represented by the black symbols are in good agreement with the theoretical curves derived from Eq. (14a) or (14b). When $\alpha = 0$, as shown in Fig. 6(a), we observe an oscillation with a visibility of 0.958, indicating that the two photons as an entity behaves like a wave. When $\alpha = \pi/2$, as shown in Fig. 6(e), the detection probability remains 0.25, with a visibility of 0.073, which indicates a particle nature of the two photons. The WPS of two photons is visualized

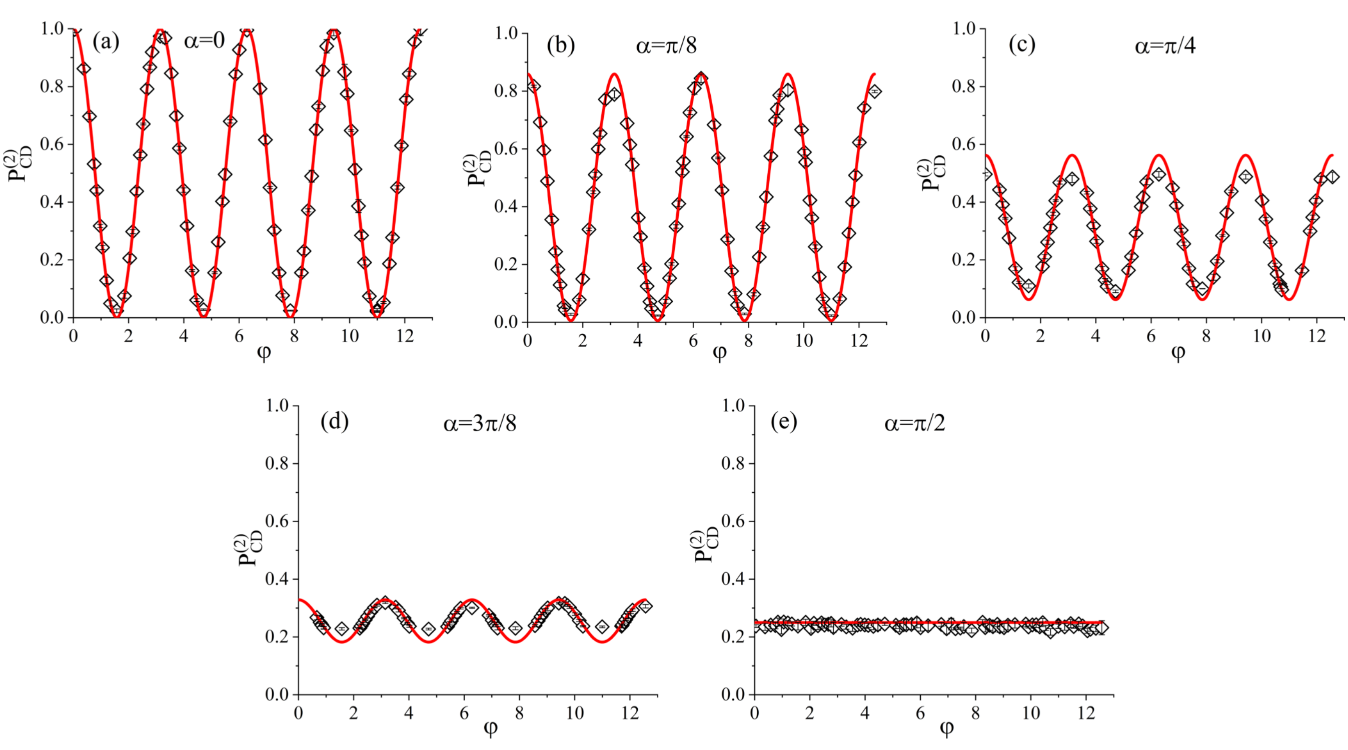

FIG. 6. The detecting probabilities $P_{CD}^{(2)}$ of the two-photon case with respect to the phase φ for different α. The black symbols are experimental results, and the lines are the corresponding theoretical ones.

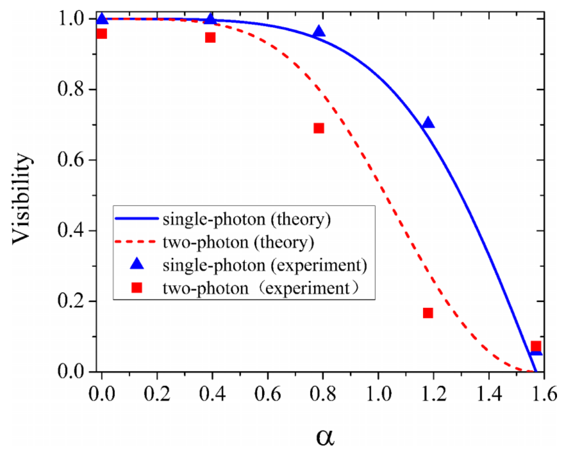

FIG. 7. The visibilities of the single-photon and two-photon interference patterns with respect to α.

in Figs. 6(a)–6(e), which show an interference pattern quite unlike the behaviors of either a wave or a particle.

After demonstrating the WPS for both single-photon and two-photon cases, we are ready to make a comparison between them. First, we observe that the oscillating frequencies of two photons against φ are two times larger than that of a single photon for $0 \leqslant \alpha < \pi/2$; in other words, the wavelength of two photons as an entity is half of that of a single photon. This result was known previously for the situation where photons exhibit a 100% wave nature when $\alpha = 0$, which is now extended to the scenario of the WPS when $0 < \alpha < \pi/2$. Second, as shown in Fig. 7, the interference visibility of two photons is always less than that of a single photon when the photons are in states of WPS with $0 < \alpha < \pi/2$, although they take the same value equal to 1 when behaving purely as a wave with $\alpha = 0$.

IV. CONCLUSION

In conclusion, we have developed a theory and carried out experiments to investigate dual behaviors of one and two photons as a wave or a particle, relying on the setup schematically sketched in Fig. 1 and detailed in Fig. 3. Our setup is far simpler than the previous one [8] in which an ancilla in a superposition state, implementation of a controlled-Hadamard gate, and proper measurement on the ancilla are required. By using our proposed setup we were able to watch purely wavelike or purely particlelike or wave-particle-superposition-like behaviors of one photon or two photons by adjusting a single classical control parameter, α, which is proportional to the reflectivity of the beam splitter which we added to the Mach-Zehnder interferometer. When we set $\alpha = 0$ both one photon and two photons exposed their 100% wave nature, with their wavelengths satisfying the relation $\lambda_2 = \lambda_1/2$, where λ_1 (λ_2) is the wavelength of the single-photon (two-photon) state. When α was chosen in the range $0 < \alpha < \pi/2$, the photon(s) was observed in wave-particle superpositions. We found that the wavelengths of both one and two photons in the wave-particle superposition states remain the same as those in the purely wave states. By continuously changing α from $\alpha = 0$ towards $\alpha = \pi/2$ a transition from wavelike to particlelike behavior occurred, which eventually became purely particlelike at $\alpha = \pi/2$. The photon wave nature is best revealed by the interference pattern with visibility depending on both the control parameter α and the number of photons considered. When $\alpha = 0$, the interference visibilities are equal to 1, and in the range of $0 < \alpha < \pi/2$, they decrease with increasing α, independent of the number of photons. However, the interference visibility in the two-photon case is always lower than that in the one-photon case. All the experimental findings agree perfectly with the theoretical predictions, certifying the relevance of the setup we have proposed. Our scheme for a delayed-choice experiment adopts a device-independent prepare-and-measure scenario to test the HVM with purely classical control. We calculated the corresponding dimension witnesses and revealed the violation of the linear dimension witness in some range of parameters, demonstrating the impossibility of HVMs. Although in this work we considered photons, similar results would also hold for matter particles.

ACKNOWLEDGMENTS

We are grateful to Profs. X.-Y. Xu and C.-F. Li for useful discussions and suggestions. For this work Z.-X.M., D.-Y.D., R.-D.M., and Y.-J.X. are supported by the National Natural Science Foundation (China) under Grants No. 11974209 and No. 12274257, the Taishan Scholar Project of Shandong Province (China) under Grant No. tsqn201812059, and the Youth Technological Innovation Support Program of Shandong Provincial Colleges and Universities under Grant No. 2019KJJ015. W.-W.P. is supported by the Anhui Provincial Natural Science Foundation under Grant No. 2208085QA13. Q.-Q.W. acknowledges support from the China Postdoctoral Science Foundation (Grant No. 2021M703108) and the National Natural Science Foundation of China (Grant No. 12204468).

[1] N. Bohr, The quantum postulate and the recent development of atomic theory, Nature (London) **121**, 580 (1928).

[2] C. Davisson and L. H. Germer, Diffraction of electrons by a crystal of nickel, Phys. Rev. **30**, 705 (1927).

[3] I. Estermann and O. Stern, Beugung von molekularstrahlen, Z. Phys. **61**, 95 (1930).

[4] H. Rauch, W. Treimer, and U. Bonse, Test of a single crystal neutron interferometer, Phys. Lett. A **47**, 369 (1974).

[5] C. Jönsson, Elektroneninterferenzen an mehreren kunstlich hergestellten feinspalten, Z. Phys. **161**, 454 (1961).

[6] J. A. Wheeler, *Quantum Theory and Measurement* (Princeton University Press, Princeton, NJ, 1984).

[7] T. Hellmuth, H. Walther, A. Zajonc, and W. Schleich, Delayed-choice experiments in quantum interference, Phys. Rev. A **35**, 2532 (1987).

[8] R. Ionicioiu and D. R. Terno, Proposal for a Quantum Delayed-Choice Experiment, Phys. Rev. Lett. **107**, 230406 (2011).
[9] J. S. Tang, Y. L. Li, X. Y. Xu, G. Y. Xiang, C. F. Li, and G. C. Guo, Realization of quantum Wheeler's delayed-choice experiment, Nat. Photonics **6**, 600 (2012).
[10] A. Peruzzo, P. Shadbolt, N. Brunner, S. Popescu, and J. L. O' Brien, A quantum delayed-choice experiment, Science **338**, 634 (2012).
[11] S. S. Roy, A. Shukla, and T. S. Mahesh, NMR implementation of a quantum delayed-choice experiment, Phys. Rev. A **85**, 022109 (2012).
[12] R. Auccaise, R. M. Serra, J. G. Filgueiras, R. S. Sarthour, I. S. Oliveira, and L. C. Céleri, Experimental analysis of the quantum complementarity principle, Phys. Rev. A **85**, 032121 (2012).
[13] F. Kaiser, T. Coudreau, P. Milman, D. B. Ostrowsky, and S. Tanzilli, Entanglement-enabled delayed choice experiment, Science **338**, 637 (2012).
[14] P. Shadbolt, J. C. F. Mathews, A. Laing, and J. L. O'Brien, Testing foundations of quantum mechanics with photons, Nat. Phys. **10**, 278 (2014).
[15] X. S. Ma, J. Kofler, A. Qarry, N. Tetik, T. Scheidl, R. Ursin, S. Ramelow, T. Herbst, L. Ratschbacher, A. Fedrizzi, T. Jennewein, and A. Zeilinger, Quantum erasure with causally disconnected choice, Proc. Natl. Acad. Sci. USA **110**, 1221 (2013).
[16] H. Yan, K. Liao, Z. Deng, J. He, Z. Y. Xue, Z. M. Zhang, and S. L. Zhu, Experimental observation of simultaneous wave and particle behavior in a narrowband single-photon wave packet, Phys. Rev. A **91**, 042132 (2015).
[17] T. Xin, H. Li, B. X. Wang, and G. L. Long, Realization of an entanglement-assisted quantum delayed-choice experiment, Phys. Rev. A **92**, 022126 (2015).
[18] S. B. Zheng, Y. P. Zhong, K. Xu, Q. J. Wang, H. Wang, L. T. Shen, C. P. Yang, J. M. Martinis, A. N. Cleland, and S. Y. Han, Quantum Delayed-Choice Experiment with a Beam Splitter in a Quantum Superposition, Phys. Rev. Lett. **115**, 260403 (2015).
[19] K. Liu, Y. Xu, W. Wang, S. B. Zheng, T. Roy, S. Kundu, M. Chand, A. Ranadive, R. Vijay, Y. Song, L. Duan, and L. Y. Sun, A twofold quantum delayed-choice experiment in a superconducting circuit, Sci. Adv. **3**, e1603159 (2017).
[20] F. Vedovato, C. Agnesi, M. Schiavon, D. Dequal, L. Calderaro, M. Tomasin, D. G. Marangon, A. Stanco, V. Luceri, G. Bianco, G. Vallone, and P. Villoresi, Extending Wheeler's delayed-choice experiment to space, Sci. Adv. **3**, e1701180 (2017).
[21] R. Chaves, G. B. Lemos, and J. Pienaar, Causal Modeling the Delayed-Choice Experiment, Phys. Rev. Lett. **120**, 190401 (2018).
[22] Q. Guo, W. J. Zhang, G. Li, T. C. Zhang, H. F. Wang, and S. Zhang, Modified quantum delayed-choice experiment without quantum control or entanglement assistance, Phys. Rev. A **104**, 022210 (2021).
[23] E. Polino, I. Agresti, D. Poderini, G. Carvacho, G. Milani, G. B. Lemos, R. Chaves, and F. Sciarrino, Device-independent test of a delayed choice experiment, Phys. Rev. A **100**, 022111 (2019).
[24] H. L. Huang, Y. H. Luo, B. Bai, Y.-H. Deng, H. Wang, Q. Zhao, H.-S. Zhong, Y.-Q. Nie, W.-H. Jiang, X.-L. Wang, J. Zhang, L. Li, N. L. Liu, T. Byrnes, J. P. Dowling, C. Y. Lu, and J. W. Pan, Compatibility of causal hidden-variable theories with a delayed-choice experiment, Phys. Rev. A **100**, 012114 (2019).
[25] S. Yu, Y. N. Sun, W. Liu, Z. D. Liu, Z. J. Ke, Y. T. Wang, J. S. Tang, C. F. Li, and G. C. Guo, Realization of a causal-modeled delayed-choice experiment using single photons, Phys. Rev. A **100**, 012115 (2019).
[26] K. Wang, D. R. Terno, Č. Brukner, S. N. Zhu, and X. S. Ma, Controlling wave-particle duality with entanglement between single-photon and bell states, Phys. Rev. A **106**, 053715 (2022).
[27] A. C. Elitzur and L. Vaidman, Quantum mechanical interaction-free measurements, Found. Phys. **23**, 987 (1993).
[28] P. Kwiat, H. Weinfurter, T. Herzog, A. Zeilinger, and M. A. Kasevich, Interaction-Free Measurement, Phys. Rev. Lett. **74**, 4763 (1995).
[29] P. G. Kwiat, A. G. White, J. R. Mitchell, O. Nairz, G. Weihs, H. Weinfurter, and A. Zeilinger, High-Efficiency Quantum Interrogation Measurements via the Quantum Zeno Effect, Phys. Rev. Lett. **83**, 4725 (1999).
[30] S. Thomas, C. Kohstall, P. Kruit, and P. Hommelhoff, Semitransparency in interaction-free measurements, Phys. Rev. A **90**, 053840 (2014).
[31] Y. Zhou and M. H. Yung, Interaction-free measurement as quantum channel discrimination, Phys. Rev. A **96**, 062129 (2017).
[32] A. E. Turner, C. W. Johnson, P. Kruit, and B. J. McMorran, Interaction-Free Measurement with Electrons, Phys. Rev. Lett. **127**, 110401 (2021).
[33] A. M. Pălici, T.-A. Isdrailă, S. Ataman, and R. Ionicioiu, Interaction-free imaging of multipixel objects, Phys. Rev. A **105**, 013529 (2022).
[34] J. S. Tang, Y. L. Li, C. F. Li, and G. C. Guo, Revisiting Bohr's principle of complementarity with a quantum device, Phys. Rev. A **88**, 014103 (2013).
[35] R. Ionicioiu, T. Jennewein, R. B. Mann, and D. R. Terno, Is wave-particle objectivity compatible with determinism and locality? Nat. Commun. **5**, 4997 (2014).
[36] P. J. Coles, J. Kaniewski, and S. Wehner, Equivalence of wave-particle duality to entropic uncertainty, Nat. Commun. **5**, 5814 (2014).
[37] R. Ionicioiu, R. B. Mann, and D. R. Terno, Determinism, Independence, and Objectivity are Incompatible, Phys. Rev. Lett. **114**, 060405 (2015).
[38] X. S. Ma, J. Kofler, and A. Zeilinger, Delayed-choice gedanken experiments and their realizations, Rev. Mod. Phys. **88**, 015005 (2016).
[39] A. S. Rab, E. Polino, Z.-X. Man, N. Ba An, Y.-J. Xia, N. Spagnolo, R. Lo Franco, and F. Sciarrino, Entanglement of photons in their dual wave-particle nature, Nat. Commun. **8**, 915 (2017).
[40] K. Wang, Q. Xu, S. Zhu, and X. S. Ma, Quantum wave-particle superposition in a delayed-choice experiment, Nat. Photonics **13**, 872 (2019).
[41] X. Chen, Y. Deng, S. Liu, T. Pramanik, J. Mao, J. Bao, C. Zhai, T. Dai, H. Yuan, J. Guo, S. M. Fei, M. Huber, B. Tang, Y. Yang, Z. Li, Q. He, Q. H. Gong, and J. Wang, A generalized multipath delayed-choice experiment on a large-scale quantum nanophotonic chip, Nat. Commun. **12**, 2712 (2021).
[42] J. Jacobson, G. Björk, I. Chuang, and Y. Yamamoto, Photonic de Broglie Waves, Phys. Rev. Lett. **74**, 4835 (1995).
[43] L. Mandel, Quantum effects in one-photon and two-photon interference, Rev. Mod. Phys. **71**, S274 (1999).

[44] B. H. Liu, F. W. Sun, Y. X. Gong, Y. F. Huang, Z. Y. Ou, and G. C. Guo, Demonstration of the three-photon de Broglie wavelength by projection measurement, Phys. Rev. A **77**, 023815 (2008).

[45] B. H. Liu, F. W. Sun, Y. X. Gong, Y. F. Huang, G. C. Guo, and Z. Y. Ou, Four-photon interference with asymmetric beam splitters, Opt. Lett. **32**, 1320 (2007).

[46] P. Walther, J. W. Pan, M. Aspelmeyer, R. Ursin, S. Gasparoni, and A. Zeilinger, De Broglie wavelength of a non-local four-photon state, Nature (London) **429**, 158 (2004).

[47] J. Bowles, M. T. Quintino, and N. Brunner, Certifying the Dimension of Classical and Quantum Systems in a Prepare-and-Measure Scenario with Independent Devices, Phys. Rev. Lett. **112**, 140407 (2014).

[48] R. Gallego, N. Brunner, C. Hadley, and A. Acín, Device-Independent Tests of Classical and Quantum Dimensions, Phys. Rev. Lett. **105**, 230501 (2010).